Docking Studies on a New Human Immodeficiency Virus Integrase−Mg−DNA Complex: Phenyl Ring Exploration and Synthesis of 1*H*-Benzylindole Derivatives through Fluorine Substitutions

Stefania Ferro, Laura De Luca, Maria Letizia Barreca, Nunzio Iraci, Sara De Grazia, Frauke Christ, Myriam Witvrouw, Zeger Debyser, and Alba Chimirri*

Dipartimento Farmaco-Chimico, Università di Messina, Viale Annunziata, 98168 Messina, Italy, Dipartimento di Chimica e Tecnologia del Farmaco, Via del Liceo 1, 06123 Perugia, Italy, Molecular Medicine, Katholieke Universiteit Leuven, 3000 Leuven, Belgium, and IRC KULAK, Kapucijnenvoer 33, B-3000 Leuven, Flanders, Belgium

Received July 24, 2008

A new model of HIV-1 integrase−Mg−DNA complex that is useful for docking experiments has been built. It was used to study the binding mode of integrase strand transfer inhibitor **1** (CHI-1043) and other fluorine analogues. Molecular modeling results prompted us to synthesize the designed derivatives which showed potent enzymatic inhibition at nanomolar concentration, high antiviral activity, and low toxicity. Microwave assisted organic synthesis (MAOS) was employed in several steps of the synthetic pathway, thus reducing reaction times and improving yields.

Introduction

Integrase (IN[a]) is one of the three human immunodeficiency virus type 1 (HIV-1) enzymes that, together with the reverse transcriptase (RT) and protease (PR), allows the virus to reproduce itself after infecting the host cell. IN inserts a double stranded DNA copy of the viral RNA genome into the chromosomes of an infected cell through two separate catalytic steps: in the "3′-processing" (3′-P) reaction, IN removes the terminal GT dinucleotides from each LTR (long-terminal repeat) 3′ end, while in the "strand transfer" (ST) reaction the two newly processed 3′-viral DNA ends are joined to the cellular DNA.[2] The integration reaction is completed by the removal of the two unpaired nucleotides at the 5′-end of the viral DNA and by the repair of the single stranded gaps created between the viral and target DNA. HIV-1 IN is composed of a single polypeptide chain that folds into three functional domains[3] and belongs to the polynucleotidyl transferase superfamily. The active site is located in the catalytic domain and is composed of two Asp residues and one Glu in the conserved D,D(35)E motif, each of which is required for catalysis. Moreover, it has long been established that divalent metal ions are essential in the active site for the hydrolytic phosphoryl transfer reactions.[4,5] The HIV-1 IN crystal structures available to date show a single binding site for Mg^{2+} or Mn^{2+}, whereas both biochemical and structural studies offer a plausible two-metal model for the catalytic center of IN. In fact, because a second metal has been observed in an avian sarcoma virus (ASV) IN crystal structure[6] and because of the two-metal structure for polynucleotide transferases,[5,7] it has been proposed that the second metal is only sequestered into the active site after HIV-1 integrase binds its DNA substrate(s).[8,9] Despite the unique role of IN in the viral replication process, to date, only one active drug against this enzyme, raltegravir, has received FDA approval.[10] Raltegravir belongs to the family of integrase strand transfer inhibitors (INSTIs), which represent the major leads in the development of anti-HIV-1 IN drugs. These molecules have been shown to specifically inhibit the DNA ST step[11] of integration by sequestering the metal ions bound in the active site of the enzyme;[8,9] moreover, it has been demonstrated that they bind to IN after the protein has formed a complex with target DNA.[12] In fact, β-diketo acids[11] (DKAs) and their derivatives[13] were the first INSTIs to display potent antiviral activity via IN inhibition. Unfortunately, there is a lack of detailed structural information about the three-domain protein structure and the interaction between IN and its substrates, and consequently structure-based design of novel HIV-1 IN inhibitors is currently hampered. To solve this problem, we previously constructed a model of the full-length HIV-1 integrase dimmer by assembling the experimentally determined structures of the single domains.[14] The three-domain protein−viral DNA complex was also generated through an automated docking algorithm (pdb code 1WKN[14]) followed by dynamic studies.[15] At the same time it was suggested that the Tn5 transposase (Tnp) could be considered an excellent surrogate model for IN,[16] and in a recent paper we reported that its X-ray crystal structure[17] can be used in docking and molecular dynamic studies to predict binding modes of HIV-1 INSTIs. [18,19]

Chart 1. Chemical Structure of Compound **1**

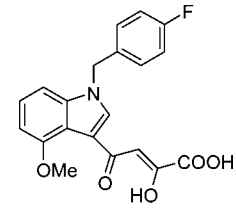

In addition, we used a ligand-based approach to generate three-dimensional pharmacophore models for HIV-1 integrase inhibitors,[20,1] which led to the discovery of some 4-[1-(4-fluorobenzyl)-1*H*-indol-3-yl]-2-hydroxy-4-oxobut-2-enoic acids as potent anti-HIV agents able to specifically inhibit the ST step of integration at nanomolar concentration. In particular, we discovered the potent derivative **1** (Chart 1) that displayed the best anti-HIV activity from this series, thus holding promise for further development.[1] The combination of these different computational strategies allowed us to generate now a novel

* To whom correspondence should be addressed. Phone: (++39) 0906766412. Fax: (++39) 0906766402. E-mail: chimirri@pharma.unime.it.

[a] Abbreviations: HIV-1, human immunodeficiency virus type 1; IN, integrase; MAOS, microwave assisted organic synthesis; RT, reverse transcriptase; PR, protease; 3′-P, 3′-processing; ST, strand transfer; LTR, long-terminal repeat; ASV, avian sarcoma virus; DKA, diketo acids; Tnp, transposase; raltegravir, *N*-(4-fluorobenzyl)-5-hydroxy-1-methyl-2-(1-methyl-1-{[(5-methyl-1,3,4-oxadiazol-2-yl)carbonyl]amino}ethyl)-6-oxo-1,6-dihydropyrimidine-4-carboxamide; elvitegravir, 6-(3-chloro-2-fluorobenzyl)-1-(3-hydroxy-2-methylpropyl)-7-methoxy-4-oxo-1,4-dihydroquinoline-3-carboxylic acid.

10.1021/jm8009266 CCC: $40.75
Published on Web 12/23/2008

HIV-1 integrase−Mg−DNA model that is useful for docking experiments. In this work it was used for the optimization of our lead **1** through the design of a new series of its fluorine analogues whose synthesis and biological evaluations are also reported herein.

Results and Discussion

Docking Studies and Design. We considered two IN−Mg−DNA ternary complexes (1WKN[14,15] and 1ZA9[21]) to be of interest in order to create a new complex. 1WKN was chosen because of the presence in its active site of both the two important Mg^{2+} ions opportunely chelated by the D64, D16, and E152 (conserved D,D(35)E motif) required for catalysis. Whereas the complex 1ZA9 was selected because even if it lacks of one Mg^{2+} ion, it nevertheless shows a viral DNA-binding obtained utilizing the already solved Tn5 transposase crystal structure as template to position the viral DNA into the IN active site. This binding mode of viral DNA was considered by us to be more appropriate than that of the 1WKN obtained by docking studies. Considering these findings, we superimposed these two IN−Mg−DNA ternary complexes (1WKN and 1ZA9) to obtain a new model that presents a complete core domain with two cations opportunely chelated by DDE motif, and a viral DNA oriented in similar way to Tn5 transposase (see Experimental Section).

This model, which was subsequently optimized by a minimization procedure, was considered to be very useful for the structure-based design and was used as template to perform docking studies with the Gold program.[22,23] First of all, we considered our most active compound **1** (Chart 1) that has been shown to selectively inhibit the IN strand transfer step (ST)[1] and likely acts like other potent IN inhibitors, namely by chelating the metal ions bound in the active site of the enzyme. The best docking pose of **1** was optimized by an energy minimization procedure using Macromodel software (see Experimental Section for details), and the result is shown in Figure 1. In this orientation the diketo acid moiety is able to interact with the two divalent ions in the active site, in perfect agreement with the proposed mechanism of action for INSTIs. Docking results also revealed the presence of a large hydrophobic cavity defined by nonpolar residues L68, I73, V75, L158, and I162 and occupied by the inhibitor 4-fluorophenyl ring of the inhibitor (Figure 1). The importance of the hydrophobic nature of the 4-fluorophenyl ring for **1** and for the most important INSTIs has been highlighted in our previous ligand-based studies that led to the generation of three-dimensional pharmacophore models (see Figure 2, feature Y). Furthermore, **1** creates important contacts with some amino acids known to be critical for DNA binding (e.g., K159, E152)[24−26] or to be associated with resistance to INSTIs.[27] In particular, our inhibitor shows close interaction with residues T66 and N155, whose mutations are capable of causing reduced sensitivity to a wide range of IN inhibitors;[11,24,28,29] such an effect might be explained considering that these two residues surrounding the above-described hydrophobic pocket and their mutations might thus influence the INSTI binding. To confirm our derivative **1** docking results, its "predicted" conformation (i.e., bound to IN) was mapped onto two previously developed pharmacophore models. Figure 2A shows the superimposition of the **1** docking pose in the quantitative HypoGen model, and interestingly, the selected pose was able to perfectly fit the model with a best estimated for activity level of 0.05 μM, close to the experimental value of 0.14 ± 0.11 μM obtained on strand-transfer step. Figure 2B shows the superimposition of the **1** docking pose in the qualitative HipHop model, in which the compound orients itself

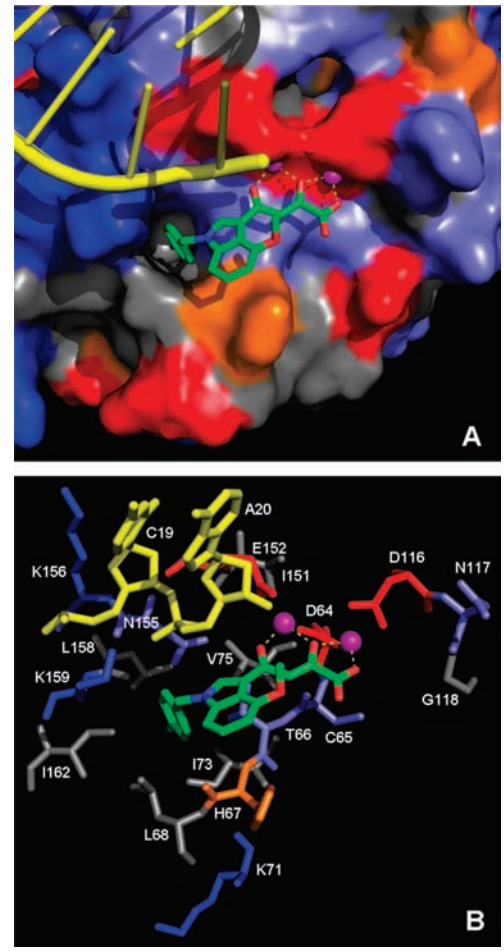

Figure 1. (A) Compound **1** (green) in the IN−Mg−DNA active site. The divalent metal ions are shown as purple spheres, while the viral DNA is depicted in yellow. Protein surface is colored as follows: basic residues, blue; acidic residues, red; polar residues, violet; nonpolar residues, gray; aromatic residues, orange. (B) INSTI **1** (yellow) and amino acids lying within 5 Å from the docked compound. Color codes as in the previous image. Yellow dashed lines represent coordination to the metal ions, highlighting the two-metal binding model for our INSTI. This figure was prepared using the PyMOL program.[39]

in the same mode engaged in the quantitative HypoGen model. We considered these results to be very important to validate our docking results, highlighting a good correlation between structure- and ligand-based approaches and the plausibility of the suggested binding mode. The evidence of a large hydrophobic cavity (about 46 Å^3) in the INSTI binding site in which the 4-F-phenyl ring is inserted suggested the design of new compounds, by moving a fluorine atom in all positions of the phenyl moiety (**15**−**16**, **26**, **27**) and by introducing two (**17**−**22**, **28**−**33**) or three (**23**−**25**, **34**−**36**) substituents on the same ring. This idea was supported by the multipresence of halogen atoms in potent IN inhibitors such as the 6-(3-chloro-2-fluorobenzyl)-1-(3-hydroxy-2-methylpropyl)-7-methoxy-4-oxo-1,4-dihydroquinoline-3-carboxylic acid (GS-9137)[30] and also by considering the importance of the fluorine atom on the binding affinity in protein−ligand complexes, which frequently leads to an enhancement of molecule binding affinity.[31] As a consequence of the docking results for the new potential INSTIs, showing a binding mode in common with that of derivative **1** (Figure 3) and comparable with docking values (i.e., the fitness scores), we therefore planned the synthesis of the designed 1*H*-benzylindole derivatives bearing one or more fluorine atoms on the different positions of the benzyl moiety.

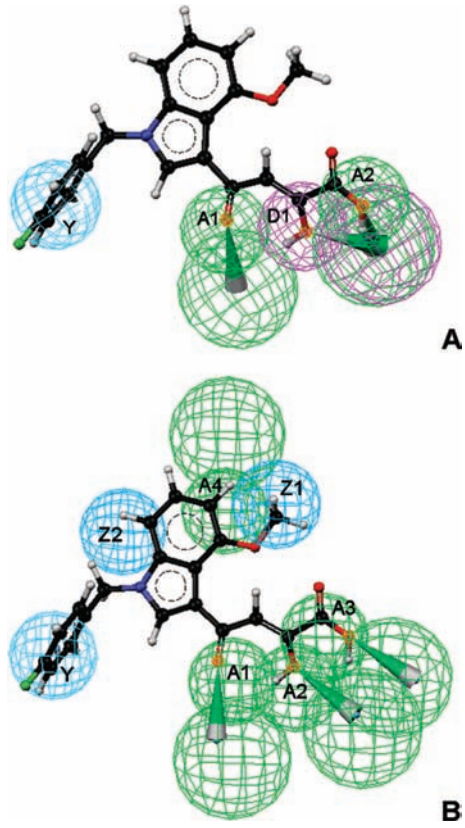

Figure 2. Best docking pose of **1** mapped on (A) 3D quantitative pharmacophore model by HypoGen (A1 and A2, hydrogen-bond acceptor, green; D1, hydrogen-bond donor, magenta; Y, hydrophobic aromatic, cyan) and (B) 3D qualitative pharmacophore model by HipHop (A1−A4, hydrogen-bond acceptor, green; Z1 and Z2, hydrophobic aliphatic, blue; Y, hydrophobic aromatic, cyan).

Chemistry. Our initial method for the previously reported synthesis[1,20] of β-hydroxydiketo acid derivatives was optimized by the application of microwave-assisted technology in the various steps of the synthetic approach, thereby increasing the yields and reducing the reaction times as well as having more selective reactions and using less solvent. The synthetic pathway followed for the preparation of the new benzyl-1*H*-indole derivatives **26**−**36** is depicted in Scheme 1. Thus, commercially available 4-methoxy-1*H*-indole (**2**) was reacted with acetyl chloride in the presence of a slight excess of diethylaluminum chloride to give intermediates **3**. While the reaction takes in 2 h under the conventional method, it requires only 10 min using the microwave assisted organic synthesis (MAOS). The obtained intermediate **3** was then N-alkylated by treatment with the suitable benzyl bromide and a small amount of sodium hydride. Under the "classical" method, the reaction was performed in 30 min, whereas when microwave irradiation was applied, this step was carried out in only 5 min and used less solvent. The synthesis of derivatives **15**−**25** was achieved by coupling 3-acetyl-4-methoxy-1-benzyl-1*H*-indoles with diethyl oxalate in the presence of a catalytic amount of sodium methoxide. The reaction was highly efficient under microwave irradiation (only 4 min). These compounds were then hydrolyzed in basic medium to provide the corresponding arylhydroxyketo acids **26**−**36**. Both analytical and spectral data of all synthesized compounds are in full agreement with the proposed structures.

Biological Activity. All the synthesized diketo acid derivatives (**26**−**36**) and all the diketo esters (**15**−**25**) that also showed good results in molecular modeling studies were tested for their inhibitory effect on IN enzymatic activity and against HIV-1 replication (Table 1). To determine the susceptibility of the HIV-1 integrase enzyme toward synthesized compounds, we used enzyme-linked immunosorbent assays as described previously.[32] However, their inhibitory effect on the HIV-induced

Scheme 1[a]

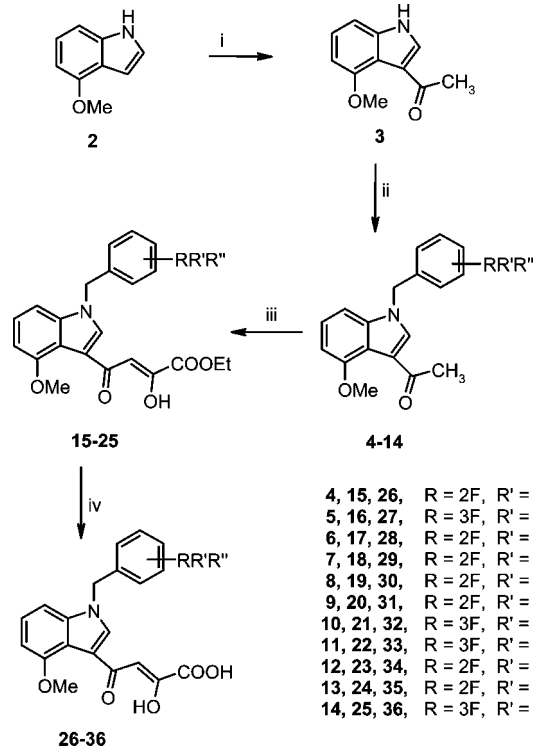

4, 15, 26, R = 2F, R' = R" = H,
5, 16, 27, R = 3F, R' = R" = H,
6, 17, 28, R = 2F, R' = 3F, R" = H,
7, 18, 29, R = 2F, R' = 4F, R" = H,
8, 19, 30, R = 2F, R' = 5F, R" = H,
9, 20, 31, R = 2F, R' = 6F, R" = H,
10, 21, 32, R = 3F, R' = 4F, R" = H,
11, 22, 33, R = 3F, R' = 5F, R" = H,
12, 23, 34, R = 2F, R' = 3F, R" = 4F,
13, 24, 35, R = 2F, R' = 3F, R" = 6F,
14, 25, 36, R = 3F, R' = 4F, R" = 5F

[a] Reagents and conditions: (i) Et_2AlCl, CH_2Cl_2, 0 °C, 30 min, AcCl, 50°C, 10 min, 100 W; (ii) $ArCH_2Br$, NaH, DMF, 50°C, 5 min, 100 W; (iii) diethyl oxalate, dry CH_3ONa, THF, two separated steps under the same conditions, 50°C, 2 min, 250 W; (iv) 2 N NaOH, MeOH, room temp, 1.5 h.

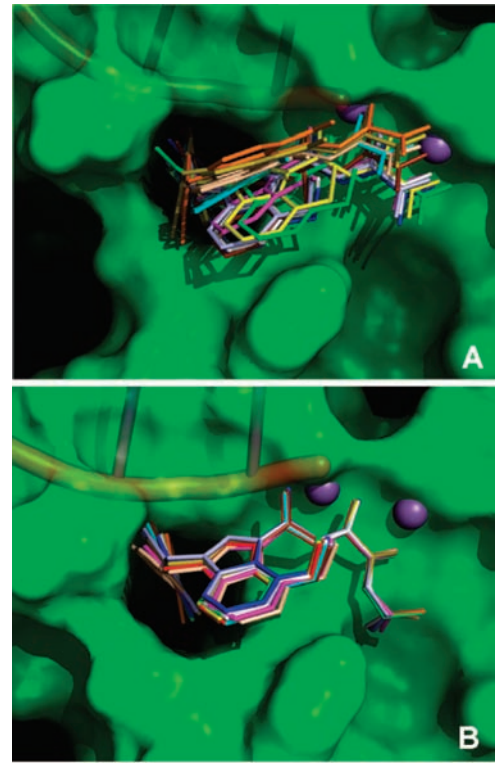

Figure 3. Best docking results in the IN−Mg−DNA active site for compounds **26**−**36** (A) and for **15**−**25** (B).

Table 1. Inhibition of HIV-1 Integrase Enzymatic Activity, Replication of HIV-1 (IIIB), and Cytotoxicity in MT-4 Cells[a]

	IN enzymatic activity, IC_{50} (μM)		activity in MT-4 cells		
compd	overall[b]	ST[c]	HIV-1[d] EC_{50} (μM)	cytotoxicity[e] CC_{50} (μM)	SI[f]
15	0.38 ± 0.07	0.72 ± 0.23	1.40 ± 0.51	63.33 ± 11.91	45.3
16	0.30 ± 0.00	2.26 ± 1.43	2.21 ± 0.50	63.21 ± 1.00	28.5
17	0.005 ± 0.00	0.012 ± 0.03	1.90 ± 0.07	21.11 ± 11.43	11.1
18	0.11 ± 0.007	0.67 ± 0.41	1.95 ± 0.17	65.48 ± 36.30	33.7
19	1.41 ± 0.07	0.40 ± 0.11	3.15 ± 0.75	41.23	13.1
20	0.36 ± 0.09	0.07 ± 0.02	2.04 ± 0.05	>63.41	>31.1
21	26.45 ± 8.71	1.56 ± 0.34	80.09 ± 0.34	>125	>2
22	1.52 ± 0.15	2.74 ± 0.33	5.94 ± 2.83	>34.7	>5.8
23	3.01 ± 1.32	1.15 ± 0.26	3.15 ± 1.23	>42.7	>13
24	0.17 ± 0.02	0.82 ± 0.04	4.84 ± 3.26	40,49 ± 19,86	8.4
25	2.0 ± 0.50	1.41 ± 0.38	3.96 ± 0.63	33.40 ± 3,00	8.4
26	0.07 ± 0.00	0.04 ± 0.01	0.31 ± 0.09	70.5 ± 24.18	228
27	0.03 ± 0.00	0.03 ± 0.00	0.38 ± 0.22	65.82 ± 2.82	175
28	0.01 ± 0.00	0.12 ± 0.05	0.26 ± 0.07	>17.53	>68.7
29	0.01 ± 0.008	0.02 ± 0.002	0.41 ± 0.03	20.81 ± 16.11	50.7
30	0.05 ± 0.00	0.02 ± 0.003	0.41 ± 0.17	46.24 ± 16.29	112.8
31	0.13 ± 0.03	0.08 ± 0.008	0.41 ± 0.03	44.28 ± 4.13	108
32	0.42 ± 0.16	0.60 ± 0.16	2.8 ± 0.28	70.95 ± 1.63	25
33	0.44 ± 0.08	0.24 ± 0.02	2.78 ± 2.41	29.52 ± 4.53	10.6
34	0.14 ± 0.01	0.28 ± 0.05	1.15 ± 0.71	22.78 ± 10.30	19.9
35	0.13 ± 0.02	0.16 ± 0.02	0.65 ± 0.07	49.35 ± 0.92	75.5
36	0.06 ± 0.02	0.10 ± 0.003	2.21 ± 0.34	23.33 ± 2.81	10.5
1 (CHI 1043)	0.08 ± 0.003	0.14 ± 0.11	0.59 ± 0.38	41.1 ± 16.7	70

[a] All data represent average results ± SD. [b] Concentration required to inhibit the in vitro overall integrase activity by 50%. [c] Concentration required to inhibit the in vitro strand transfer step by 50%. [d] Effective concentration required to reduce HIV-1-induced cytopathic effect by 50% in MT-4 cells. [e] Cytotoxic concentration to reduce MT-4 cell viability by 50%. [f] Selectivity index: ratio CC_{50}/EC_{50}.

cytopathic effect (CPE) in human lymphocyte MT-4 cell culture was determined by the MT-4/MTT-assay.[33] All diketo acids (**26**−**36**) showed activity at nanomolar concentrations in the overall integration reaction and in the more specific ST assay, and seven of them were more active than the lead compound **1**. The corresponding esters (**15**−**25**) were generally less active than diketo acids probably for their lower ability to sequester the metal ions bound in the active site of the enzyme. Considering the position of the fluorine atom, the ortho substitution seems preferable. In fact, the most active derivatives on ST assay generally present one fluorine atom at the 2-position. Some esters proved to be potent inhibitors, particularly if disubstituted (i.e., **17**, **20**). Interestingly, all derivatives proved to be active also in cell tests, and **26**, **27**, **30**, **31** exhibited very low toxicity with SI > 100.

Conclusions

A new model of HIV-1 IN−Mg−DNA complex has been built. A combined ligand-based and structure-based approach was used for the design of potent IN inhibitors. While investigating the importance of the substitution on the phenyl ring, we identified a number of compounds structurally related to **1** that behave as potent IN inhibitors at nanomolar concentration with a very low toxicity. These results confirm the importance of occupying the large hydrophobic cavity present in the INSTI site and underline the role of computational methodologies in medicinal chemistry research.

Experimental Section

Docking Studies. Preparation of the Target and Ligands for Docking. The IN−Mg−DNA ternary complex was built by superimposing the structures of 1WKN and 1ZA9 and aligning their DDE motif with their α carbons. 1ZA9 is a model of the integration complex based on experimental evidence, including a comparison with the homologous Tn5 transposase containing bound DNA and an analysis of DNA binding sites using Goodford's GRID.[21] 1WKN is a model of full-length HIV-1 integrase dimer viral DNA constructed by assembling the experimentally determined structures of the single domains followed by docking experiments for the orientation of viral DNA.[14,15] The core domain of 1WKN was maintained, considering that all amino acids were present and that also the two Mg ions were opportunely inserted with the DDE correctly oriented. From 1ZA9 the viral DNA was kept, which was modeled directly from Tn5 transposase coordinates.[21] To remove the worst contacts between the parts of this new complex but not to alter the architecture of the binding site, 100 steps of steepest descent minimization (OPLS-2005 force field) using GB/SA[34] model as solvation treatment were carried out by freezing the two cations and the oxygen atom of the 3′OH of adenosine−viral DNA using Macromodel program.[35] The structures of ligands were constructed using the Schrodinger Maestro[36] and were then submitted to Polak−Ribiere conjugate gradient minimization (0.0005 kJ/(Å mol) convergence). The compounds were presented in their enolic tautomeric form, since it has been clearly established that DKAs mainly exist in this form in solution, the carboxylic moiety was considered as carboxylate, and the enolic oxygen was considered as enolate given the influence of the two metal ions in the binding site.[37]

Gold. Compounds were docked to the binding site by means of CCDC's GOLD (Genetic Optimization for Ligand Docking) software, version 3.1.1.[22] The binding region for the docking study was defined as a 10 Å radius sphere centered on the centroid of the two metal ions. One-hundred genetic algorithm (GA) runs were performed for each compound, and 10 ligand bumps were allowed in an attempt to account for mutual ligand/target fit. For each of the GA runs, a maximum number of 100 000 operations were performed on a population of 100 individuals with a selection pressure of 1.1. The number of islands was set to 5, with a niche size of 2. The weights of crossover, mutation, and migration were set to 95, 95, and 10, respectively. The scoring function, GoldScore, implemented in GOLD was used to rank the docking positions of compounds, which were clustered together when differing by more than 2 Å in rmsd. The best ranking clusters for each of the compounds were selected.

Minimization Process. All IN/DNA/ligand complexes obtained by docking studies were minimized using a two-step procedure. In a first step 1000 iterations of SD minimization were carried out by freezing the two cations and the 3′-OH oxygen, while in a second step 1000 iterations of Polak−Ribiere conjugate gradient unrestrained minimization were performed. Minimization of complexes was performed using the OPLS-2005[34] force field and the GB/SA model[38] as solvation treatment.

Synthesis. See Supporting Information.

Acknowledgment. We acknowledge technical assistance at the Katholieke Universiteit Leuven of Martine Michiels (integrase assays), Linda Desender (protein purification), and Barbara Van Remoortel (HIV assays). This work was supported by THINC project (European Commission GrantHEALTH-F3-2008-201032).

Supporting Information Available: Additional experimental details and ^{1}H NMR and elemental analysis data for all compounds. This material is available free of charge via the Internet at http://pubs.acs.org.

References

(1) De Luca, L.; Barreca, M. L.; Ferro, S.; Iraci, N.; Michiels, M.; Christ, F.; Debyser, Z.; Witvrouw, M.; Chimirri, A. A refined pharmacophore model for HIV-1 integrase inhibitors: optimization of potency in the 1*H*-benzylindole series. *Bioorg. Med. Chem. Lett.* **2008**, *18*, 2891–2895.
(2) Chiu, T. K.; Davies, D. R. Structure and function of HIV-1 integrase. *Curr. Top. Med. Chem.* **2004**, *4*, 965–977.
(3) Andrake, M. D.; Skalka, A. M. Retroviral integrase, putting the pieces together. *J. Biol. Chem.* **1996**, *271*, 19633–19636.
(4) d'Angelo, J.; Mouscadet, J. F.; Desmaele, D.; Zouhiri, F.; Leh, H. HIV-1 integrase: the next target for AIDS therapy. *Pathol. Biol. (Paris)* **2001**, *49*, 237–246.
(5) Yang, W.; Steitz, T. A. Recombining the structures of HIV integrase, RuvC and RNase H. *Structure* **1995**, *3*, 131–134.
(6) Bujacz, G.; Alexandratos, J.; Wlodawer, A.; Merkel, G.; Andrake, M.; Katz, R. A.; Skalka, A. M. Binding of different divalent cations to the active site of avian sarcoma virus integrase and their effects on enzymatic activity. *J. Biol. Chem.* **1997**, *272*, 18161–18168.
(7) Beese, L. S.; Steitz, T. A. Structural basis for the 3′−5′ exonuclease activity of *Escherichia coli* DNA polymerase I: a two metal ion mechanism. *EMBO J.* **1991**, *10*, 25–33.
(8) Grobler, J. A.; Stillmock, K.; Hu, B.; Witmer, M.; Felock, P.; Espeseth, A. S.; Wolfe, A.; Egbertson, M.; Bourgeois, M.; Melamed, J.; Wai, J. S.; Young, S.; Vacca, J.; Hazuda, D. J. Diketo acid inhibitor mechanism and HIV-1 integrase: implications for metal binding in the active site of phosphotransferase enzymes. *Proc. Natl. Acad. Sci. U.S.A.* **2002**, *99*, 6661–6666.
(9) Marchand, C.; Johnson, A. A.; Karki, R. G.; Pais, G. C.; Zhang, X.; Cowansage, K.; Patel, T. A.; Nicklaus, M. C.; Burke, T. R., Jr.; Pommier, Y. Metal-dependent inhibition of HIV-1 integrase by beta-diketo acids and resistance of the soluble double-mutant (F185K/C280S). *Mol. Pharmacol.* **2003**, *64*, 600–609.
(10) www.fda.gov/bbs/topics/NEWS/2007/NEW01726.html.
(11) Hazuda, D. J.; Felock, P.; Witmer, M.; Wolfe, A.; Stillmock, K.; Grobler, J. A.; Espeseth, A.; Gabryelski, L.; Schleif, W.; Blau, C.; Miller, M. D. Inhibitors of strand transfer that prevent integration and inhibit HIV-1 replication in cells. *Science* **2000**, *287*, 646–650.
(12) Espeseth, A. S.; Felock, P.; Wolfe, A.; Witmer, M.; Grobler, J.; Anthony, N.; Egbertson, M.; Melamed, J. Y.; Young, S.; Hamill, T.; Cole, J. L.; Hazuda, D. J. HIV-1 integrase inhibitors that compete with the target DNA substrate define a unique strand transfer conformation for integrase. *Proc. Natl. Acad. Sci. U.S.A.* **2000**, *97*, 11244–11249.
(13) Johnson, A. A.; M., C.; Pommier, Y. HIV-1 IN inhibitors: a decade of research and two drugs in clinical trial. *Curr. Top. Med. Chem.* **2004**, *4*, 1059–1077.
(14) De Luca, L.; Pedretti, A.; Vistoli, G.; Barreca, M. L.; Villa, L.; Monforte, P.; Chimirri, A. Analysis of the full-length integrase−DNA complex by a modified approach for DNA docking. *Biochem. Biophys. Res. Commun.* **2003**, *310*, 1083–1088.
(15) De Luca, L.; Vistoli, G.; Pedretti, A.; Barreca, M. L.; Chimirri, A. Molecular dynamics studies of the full-length integrase−DNA complex. *Biochem. Biophys. Res. Commun.* **2005**, *336*, 1010–1016.
(16) Ason, B.; Knauss, D. J.; Balke, A. M.; Merkel, G.; Skalka, A. M.; Reznikoff, W. S. Targeting Tn5 transposase identifies human immunodeficiency virus type 1 inhibitors. *Antimicrob. Agents Chemother.* **2005**, *49*, 2035–2043.
(17) Steiniger-White, M.; Rayment, I.; Reznikoff, W. S. Structure/function insights into Tn5 transposition. *Curr. Opin. Struct. Biol.* **2004**, *14*, 50–57.
(18) Barreca, M. L.; De Luca, L.; Iraci, N.; Chimirri, A. Binding mode prediction of strand transfer HIV-1 integrase inhibitors using Tn5 transposase as a plausible surrogate model for HIV-1 integrase. *J. Med. Chem.* **2006**, *49*, 3994–3997.
(19) Barreca, M. L.; Ortuso, F.; Iraci, N.; De Luca, L.; Alcaro, S.; Chimirri, A. Tn5 transposase as a useful platform to simulate HIV-1 integrase inhibitor binding mode. *Biochem. Biophys. Res. Commun.* **2007**, *363*, 554–560.
(20) Barreca, M. L.; Ferro, S.; Rao, A.; De Luca, L.; Zappala, M.; Monforte, A. M.; Debyser, Z.; Witvrouw, M.; Chimirri, A. Pharmacophore-based design of HIV-1 integrase strand-transfer inhibitors. *J. Med. Chem.* **2005**, *48*, 7084–7088.
(21) Wielens, J.; Crosby, I. T.; Chalmers, D. K. A three-dimensional model of the human immunodeficiency virus type 1 integration complex. *J. Comput.-Aided Mol. Des.* **2005**, *19*, 301–317.
(22) *GOLD 3.1.1*; Cambridge Crystallographic Data Centre: Cambridge, U.K.
(23) Jones, G.; Willett, P.; Glen, R. C.; Leach, A. R.; Taylor, R. Development and validation of a genetic algorithm for flexible docking. *J. Mol. Biol.* **1997**, *267*, 727–748.
(24) Alves, C. N.; Marti, S.; Castillo, R.; Andres, J.; Tunon, I.; Moliner, V.; Silla, E. A quantum mechanics/molecular mechanic study of the wild-type and N155S mutant HIV-1 integrase complexed with a diketo acid. *Biophys. J.* Published online Nov 2, 2007, doi:10.1529/biophysj.107.107623.
(25) Gerton, J. L.; Ohgi, S.; Olsen, M.; DeRisi, J.; Brown, P. O. Effects of mutations in residues near the active site of human immunodeficiency virus type 1 integrase on specific enzyme−substrate interactions. *J. Virol.* **1998**, *72*, 5046–5055.
(26) Jenkins, T. M.; Esposito, D.; Engelman, A.; Craigie, R. Critical contacts between HIV-1 integrase and viral DNA identified by structure-based analysis and photo-crosslinking. *EMBO J.* **1997**, *16*, 6849–6859.
(27) Pommier, Y.; Johnson, A. A.; Marchand, C. Integrase inhibitors to treat HIV/AIDS. *Nat. Rev. Drug Discovery* **2005**, *4*, 236–248.
(28) Hazuda, D. J.; Anthony, N. J.; Gomez, R. P.; Jolly, S. M.; Wai, J. S.; Zhuang, L.; Fisher, T. E.; Embrey, M.; Guare, J. P., Jr.; Egbertson, M. S.; Vacca, J. P.; Huff, J. R.; Felock, P. J.; Witmer, M. V.; Stillmock, K. A.; Danovich, R.; Grobler, J.; Miller, M. D.; Espeseth, A. S.; Jin, L.; Chen, I. W.; Lin, J. H.; Kassahun, K.; Ellis, J. D.; Wong, B. K.; Xu, W.; Pearson, P. G.; Schleif, W. A.; Cortese, R.; Emini, E.; Summa, V.; Holloway, M. K.; Young, S. D. A naphthyridine carboxamide provides evidence for discordant resistance between mechanistically identical inhibitors of HIV-1 integrase. *Proc. Natl. Acad. Sci. U.S.A.* **2004**, *101*, 11233–11238.
(29) Fikkert, V.; Van Maele, B.; Vercammen, J.; Hantson, A.; Van Remoortel, B.; Michiels, M.; Gurnari, C.; Pannecouque, C.; De Maeyer, M.; Engelborghs, Y.; De Clercq, E.; Debyser, Z.; Witvrouw, M. Development of resistance against diketo derivatives of human immunodeficiency virus type 1 by progressive accumulation of integrase mutations. *J. Virol.* **2003**, *77*, 11459–11470.
(30) Sato, M.; Motomura, T.; Aramaki, H.; Matsuda, T.; Yamashita, M.; Ito, Y.; Kawakami, H.; Matsuzaki, Y.; Watanabe, W.; Yamataka, K.; Ikeda, S.; Kodama, E.; Matsuoka, M.; Shinkai, H. Novel HIV-1 integrase inhibitors derived from quinolone antibiotics. *J. Med. Chem.* **2006**, *49*, 1506–1508.
(31) Bohm, H. J.; Banner, D.; Bendels, S.; Kansy, M.; Kuhn, B.; Muller, K.; Obst-Sander, U.; Stahl, M. Fluorine in medicinal chemistry. *ChemBioChem* **2004**, *5*, 637–643.
(32) Busschots, K.; Voet, A.; De Maeyer, M.; Rain, J. C.; Emiliani, S.; Benarous, R.; Desender, L.; Debyser, Z.; Christ, F. Identification of the LEDGF/p75 binding site in HIV-1 integrase. *J. Mol. Biol.* **2007**, *365*, 1480–1492.
(33) Pauwels, R.; Balzarini, J.; Baba, M.; Snoeck, R.; Schols, D.; Herdewijn, P.; Desmyter, J.; De Clercq, E. Rapid and automated tetrazolium-based colorimetric assay for the detection of anti-HIV compounds. *J. Virol. Methods* **1988**, *20*, 309–321.
(34) Jorgensen, W. L.; Maxwell, D. S.; Tirado-Rives, J. Development and testing of the OPLS all-atom force field on conformational energetics and properties of organic liquids. *J. Am. Chem. Soc.* **1996**, *118*, 11225–11236.
(35) *MacroModel*, version 9.5M; Schrodinger, LLC: New York, 2007.
(36) *Maestro0*, version 8; Schrodinger, LLC: New York, 2007.
(37) Maurin, C.; Bailly, F.; Buisine, E.; Vezin, H.; Mbemba, G.; Mouscadet, J. F.; Cotelle, P. Spectroscopic studies of diketoacids−metal interactions. A probing tool for the pharmacophoric inter-metallic distance in the HIV-1 integrase active site. *J. Med. Chem.* **2004**, *47*, 5583–5586.
(38) Still, W. C.; Tempczyk, A.; Hawley, R. C.; Hendrickson, T. Semianalytical treatment of solvation for molecular mechanics and dynamics. *J. Am. Chem. Soc.* **1990**, *112*, 6127–6129.
(39) DeLano, W. L. *The PyMOL Molecular Graphics System*; DeLano Scientific LLC: San Carlos, CA; http://www.pymol.org.

JM8009266